

Article

Not peer-reviewed version

---

# Biomechanical Effects of Lower-Limb Asymmetry During Running: An OpenSim Computational Study

---

[Dan Cristian Manescu](#) \* and Andreea Maria Mănescu

Posted Date: 21 July 2025

doi: [10.20944/preprints2025071619.v1](https://doi.org/10.20944/preprints2025071619.v1)

Keywords: computational biomechanics; asymmetry; symmetry; running biomechanics; OpenSim; injury prevention; gait analysis; muscle activation



Preprints.org is a free multidisciplinary platform providing preprint service that is dedicated to making early versions of research outputs permanently available and citable. Preprints posted at Preprints.org appear in Web of Science, Crossref, Google Scholar, Scilit, Europe PMC.

Copyright: This open access article is published under a Creative Commons CC BY 4.0 license, which permit the free download, distribution, and reuse, provided that the author and preprint are cited in any reuse.

Disclaimer/Publisher's Note: The statements, opinions, and data contained in all publications are solely those of the individual author(s) and contributor(s) and not of MDPI and/or the editor(s). MDPI and/or the editor(s) disclaim responsibility for any injury to people or property resulting from any ideas, methods, instructions, or products referred to in the content.

## Article

# Biomechanical Effects of Lower-Limb Asymmetry During Running: An OpenSim Computational Study

Dan Cristian Manescu \* and Andreea Maria Mănescu

Academy of Economic Sciences Bucharest, Romania

\* Correspondence: dan.manescu@defs.ase.ro

## Abstract

Symmetry and asymmetry significantly influence running biomechanics, performance, and injury risk. Given the practical, ethical, and methodological constraints inherent in human-subject studies, computational modeling emerges as a valuable alternative for exploring biomechanical asymmetries in detail. This study systematically evaluated the biomechanical effects of lower limb asymmetry during running using computational musculoskeletal modeling in OpenSim. By simulating controlled asymmetries in limb strength, stride length, and ground reaction forces ( $\pm 5\%$  and  $\pm 10\%$ ), we quantified alterations in joint moments, ground reaction forces (GRF), and muscular activation patterns. Results demonstrated significant biomechanical deviations under asymmetric conditions, with vertical GRF decreasing by up to 15% on the weaker limb and increasing by up to 13% on the stronger limb. Peak knee joint moments increased by up to 20% on the stronger limb under pronounced asymmetry. Muscular activation of key lower limb muscles, such as the gastrocnemius and quadriceps, increased substantially (up to 25%) to compensate for mechanical imbalance. These findings clearly illustrate the detrimental impact of asymmetrical loading, emphasizing the increased injury risks associated with limb asymmetry. Computational modeling proved to be a robust, ethical, and economically viable approach, offering practical insights that can directly inform targeted training and injury-prevention interventions.

**Keywords:** computational biomechanics; asymmetry; symmetry; running biomechanics; OpenSim; injury prevention; gait analysis; muscle activation

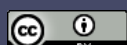
---

## 1. Introduction

Biomechanical symmetry plays a fundamental role in optimizing running efficiency, improving athletic performance, and reducing injury incidence. Recent research emphasizes that symmetrical lower limb biomechanics is associated with optimal mechanical efficiency, lower metabolic costs, and reduced susceptibility to overuse injuries. Conversely, biomechanical asymmetry, frequently arising due to anatomical variations, unilateral injuries, or training-induced imbalances, consistently contributes to altered joint kinetics, increased muscular stress, and heightened risk for chronic running-related injuries, such as stress fractures, tendinopathies, and joint disorders [1–4].

Recent studies across various sports disciplines, including football, athletics, and endurance running, have highlighted the prevalence and impact of biomechanical asymmetries resulting from sport-specific training regimens, injury histories, and habitual movement patterns. For example, football players commonly exhibit pronounced limb strength asymmetries due to repetitive unilateral kicking actions, significantly increasing injury susceptibility and potentially hindering performance optimization. Similarly, endurance runners frequently develop stride length asymmetries, often arising from chronic fatigue or previous unilateral injuries, underscoring the necessity for consistent monitoring and targeted corrective interventions [5–9].

Advancements in wearable inertial sensor technology combined with computational modeling and machine learning techniques offer promising solutions for continuous and accessible biomechanical assessments. These innovative approaches enable real-time monitoring and precise



identification of biomechanical asymmetries, facilitating proactive injury prevention and the development of highly individualized, evidence-based training and rehabilitation programs [10–13].

Although significant advancements have been made in experimental biomechanics through the use of advanced motion capture systems, electromyography (EMG), and force-plate analyses, these approaches encounter inherent practical limitations, including ethical constraints, high costs, variability in human performance, and challenges in achieving rigorous experimental control. Consequently, recent literature advocates computational musculoskeletal modeling as an ethical, controlled, and economically feasible alternative for detailed biomechanical exploration [14–17]. The strength of computational modeling and simulation has already been validated in various scientific fields beyond biomechanics, such as theoretical physics, astrophysics, and modified gravity studies, demonstrating the generalizability and robustness of numerical approaches in complex systems exploration [18,19].

Among available computational tools, OpenSim has increasingly gained prominence, demonstrating exceptional capabilities in simulating complex biomechanical scenarios and allowing precise manipulation of variables such as limb strength, stride length, and ground reaction forces under strictly controlled conditions. However, despite its growing adoption, most existing computational studies analyze isolated biomechanical parameters, leaving significant gaps in understanding the integrated impact of combined limb strength, stride length, and ground reaction force asymmetries [20–23].

To date, comprehensive computational studies addressing these combined asymmetries remain scarce, limiting our understanding of their cumulative biomechanical implications and associated injury risks. Therefore, the present study aims precisely to fill this research gap by systematically examining the biomechanical consequences of combined lower limb asymmetries during running using an advanced OpenSim musculoskeletal modeling approach. By clearly quantifying alterations in ground reaction forces, joint moments, and muscle activation patterns, this study provides novel and integrative biomechanical benchmarks essential for effective injury-prevention strategies and targeted athletic training interventions.

The originality and specific contributions of this research particularly include:

- Systematic computational analysis of the combined effects of limb strength, stride length, and ground reaction force asymmetries, an approach previously unexplored comprehensively in the literature.
- Precise quantification of biomechanical changes and compensatory mechanisms under mild ( $\pm 5\%$ ) and pronounced ( $\pm 10\%$ ) asymmetry scenarios.
- Providing detailed, replicable computational benchmarks directly applicable in athletic practice, informing targeted interventions aimed at reducing injury risks and optimizing athletic performance.

### 1.1. Theoretical Foundations

Recent literature emphasizes biomechanical symmetry as a fundamental factor influencing running performance and injury prevention. Symmetrical biomechanics are generally associated with optimized mechanical efficiency, reduced metabolic costs, and minimized injury risks in runners. Conversely, biomechanical asymmetry has consistently been linked to altered joint kinetics, increased muscular stress, and heightened risk of chronic overuse injuries. Empirical evidence underscores that runners exhibiting substantial asymmetry demonstrate greater susceptibility to injuries such as stress fractures, tendinopathies, and joint disorders due to uneven mechanical loading and muscular compensation patterns. Moreover, recent findings indicate that even subtle lower-limb asymmetries - often imperceptible in observational assessments - can induce measurable alterations in joint kinetics and neuromuscular coordination, acting as latent risk factors for cumulative overload injuries in endurance runners and field-sport athletes alike [24–27].

Numerous experimental studies have confirmed the negative impact of limb asymmetry. Research employing advanced motion capture systems, force plates, and electromyography (EMG)

has demonstrated significant correlations between asymmetrical loading patterns and increased injury incidence. It has been established that runners exhibiting asymmetrical gait patterns experience increased mechanical stress on joints, particularly the knee, ankle, and hip joints, highlighting these areas as especially vulnerable under asymmetrical loading conditions. Further investigations into muscle activation have shown that asymmetrical biomechanics prompt compensatory neuromuscular strategies, resulting in muscular imbalances, increased fatigue, and diminished neuromuscular efficiency [28–30]. Advanced analytical methods, such as Statistical Parametric Mapping (SPM), have further refined the ability to quantify subtle differences in muscle activation patterns under varying biomechanical conditions. Recent studies employing SPM demonstrate its effectiveness in distinguishing muscle recruitment differences associated with positional adjustments and comfort-oriented versus performance-oriented scenarios. Such methodological advancements are instrumental for understanding complex neuromuscular responses and optimizing training or rehabilitation interventions aimed at reducing asymmetry-related injury risks [31].

Additionally, biomechanical asymmetry can affect running economy and overall athletic performance. Studies investigating running economy have reported that even subtle biomechanical imbalances can significantly elevate metabolic energy expenditure. These findings underscore the importance of symmetry for energy-efficient running and sustained athletic performance. Further, longitudinal studies tracking athletes over extended periods have found clear links between asymmetrical biomechanics, increased fatigue rates, and reduced endurance capacity [32,33].

Computational musculoskeletal modeling, particularly through tools such as OpenSim, has emerged as a complementary research approach capable of overcoming several practical, methodological, and ethical constraints inherent in traditional experimental studies. OpenSim modeling enables detailed, controlled manipulation of biomechanical parameters, offering a precise environment for simulating a variety of hypothetical scenarios. Previous computational studies have effectively utilized OpenSim to examine lower limb biomechanics, validate experimental findings, and explore injury mechanisms and preventive strategies. Computational simulations have successfully quantified muscle contributions during running, analyzed joint load distribution, and evaluated neuromuscular adaptation under various biomechanical conditions [34,35].

Recent advancements in computational biomechanics further illustrate the potential of this approach to systematically explore scenarios difficult to replicate experimentally. Studies have effectively employed computational models to analyze complex biomechanical interactions and predict injury outcomes under diverse conditions, thereby significantly extending our understanding of injury mechanisms and prevention strategies. Validation of computational models against experimental and clinical data has reinforced their credibility and increased their applicability in biomechanical research [36,37].

Emerging research has expanded computational modeling applications to specific athletic contexts and clinical rehabilitation scenarios, enabling researchers to better understand individual differences in biomechanical responses and adaptation patterns. Such personalized biomechanical modeling holds significant promise for designing customized preventive interventions and targeted rehabilitation protocols [38].

The integration of computational methods with traditional biomechanical research significantly enhances the ability to investigate limb asymmetry comprehensively and precisely. This integrated approach provides detailed insights into the biomechanical impacts of asymmetry, offering essential knowledge for developing targeted preventive measures, optimized training protocols, and evidence-based rehabilitation practices for runners and other athletes [39,40].

Furthermore, recent advancements in computational biomechanics and wearable sensor technology have significantly enhanced the ability to detect, quantify, and monitor biomechanical asymmetries. Wearable inertial measurement units (IMUs) combined with machine learning algorithms now offer practical, real-time assessment of asymmetrical movement patterns during training and competition. These emerging methodologies provide coaches and therapists with

precise, actionable data, facilitating the development of individualized and proactive training or rehabilitation programs. Computational modeling approaches, such as the OpenSim platform used in this study, complement these technological advancements by enabling controlled, systematic exploration of biomechanical parameters. This integrated approach of technology-driven assessment and computational modeling represents a critical step forward in understanding and managing limb asymmetries, offering substantial potential to enhance athletic performance and injury prevention strategies across diverse sporting contexts [41–43].

Given these theoretical insights and recent technological advances, there remains a clear need for systematic, controlled investigations that explicitly quantify the combined effects of multiple biomechanical asymmetries (limb strength, stride length, and ground reaction forces) during running. The current study addresses this gap explicitly, utilizing computational musculoskeletal modeling in OpenSim to provide precise, reproducible benchmarks that directly inform evidence-based athletic training and injury prevention practices.

## 2. Materials and Methods

The methodological approach adopted in this study was specifically tailored to harness the capabilities of computational biomechanics, enabling a detailed examination of lower limb asymmetry during running while circumventing the limitations inherent in human-subject research. By employing state-of-the-art musculoskeletal modeling techniques and rigorously validated computational tools, we systematically evaluated biomechanical responses under controlled asymmetrical conditions. This computational framework allowed precise manipulation of key parameters, facilitating robust and reproducible insights into the complex interplay between limb asymmetry, joint mechanics, muscular function, and running performance.

The following subsections present a comprehensive account of the simulation methodology, encompassing the foundational model selection, the configuration of biomechanical variables, and the analytical procedures applied - thereby ensuring transparency and reproducibility for future research.

The three parameters selected for asymmetry analysis - limb strength, stride length, and ground reaction forces - were chosen based on their documented relevance in previous literature as critical determinants of running biomechanics and injury susceptibility. Limb strength asymmetry is often observed in athletes with a history of unilateral injuries; stride length asymmetry frequently arises due to habitual gait patterns; and ground reaction force asymmetry directly reflects disparities in mechanical loading between limbs. By independently manipulating each parameter within the simulation, our design enabled the isolation and assessment of their individual and combined biomechanical impacts.

To visually synthesize the methodological framework, Figure 1 schematically illustrates the key stages of the computational pipeline. This includes the selection of the validated OpenSim gait2392 musculoskeletal model, the definition of core biomechanical parameters (limb strength, stride length, ground reaction forces), the application of systematic asymmetrical perturbations ( $\pm 5\%$ ,  $\pm 10\%$ ), and the extraction of relevant biomechanical outputs (ground reaction forces, joint moments, and muscle activation patterns). These outputs were then subjected to rigorous statistical analysis and graphical interpretation, providing a solid foundation for biomechanical inference and actionable insights for performance enhancement and injury prevention.

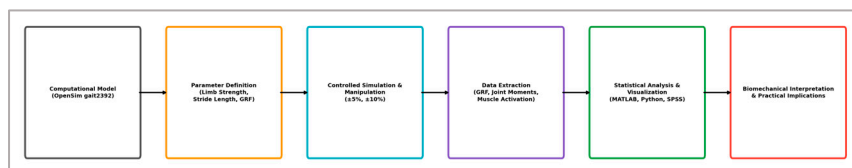


**Figure 1.** Computational workflow for analyzing biomechanical effects of lower limb asymmetry during running.

This structured methodological framework provided the foundation for rigorous analysis and biomechanical interpretation throughout the study, ensuring clarity in parameter manipulation, consistency in simulation execution, and reproducibility in biomechanical outcome assessment.

### 2.1. Computational Model

The computational modeling framework employed in this study was developed using OpenSim (version 4.4), a validated open-source musculoskeletal simulation platform widely used for quantitative analysis of human movement. OpenSim enables precise, anatomically accurate simulations by combining multibody dynamics with muscle-actuated models governed by biomechanical and neuromuscular control principles. This modeling approach facilitates high-resolution, replicable experimentation with biomechanical parameters that are otherwise difficult to manipulate in human-subject settings.

The simulations were based on the gait2392 musculoskeletal model, a standardized and extensively validated OpenSim model [44] representing an average healthy adult with a body mass of 75 kg and a height of 1.80 m. The model incorporates 23 biomechanical degrees of freedom (DOFs) and is actuated by 92 musculotendon units, enabling a physiologically realistic replication of lower limb kinetics and neuromuscular dynamics during running. Anatomical structures are accurately represented, including the pelvis, femur, tibia, fibula, and foot segments, with articulated joints parameterized for sagittal, frontal, and transverse motion.

Each musculotendon actuator in the gait2392 model is governed by a Hill-type muscle model, which accounts for force-length, force-velocity, and activation-contraction coupling dynamics, as well as tendon elasticity. Muscle-specific parameters - including optimal fiber length, tendon slack length, maximum isometric force ( $F_{max}$ ), pennation angle, and maximum contraction velocity - were retained from the original distribution and were not altered across conditions, except when explicitly defined by asymmetry scenarios. This ensured biomechanical consistency and comparability across simulation conditions.

To solve the equations of motion and simulate the forward dynamics of the system, we employed Simbody integrators with the semi-explicit Euler method, using an integration step size of 0.001 s and a numerical tolerance of 1e-6. Simulations were configured to generate 10 consecutive gait cycles under each condition, ensuring steady-state kinematics and convergence stability. No residual actuators or artificial torque sources were introduced, preserving the physiological plausibility of muscular control.

The choice of gait2392 was motivated by its wide validation in the literature, including comparisons with experimental electromyography (EMG), motion capture kinematics, and ground reaction force (GRF) data during walking and running. Previous studies have shown that gait2392 reliably predicts joint angles, net joint moments, and muscle activations with high fidelity, supporting its credibility as a computational proxy for investigating lower limb biomechanics under both symmetrical and asymmetrical conditions.

This modeling foundation enabled systematic perturbation of biomechanical parameters within a controlled, physiologically consistent simulation environment. All simulations were initialized from standardized kinematic states derived from inverse kinematics solutions of normative running data. The model's internal consistency, dynamic stability, and anatomical fidelity provided a robust platform for quantifying joint loading, neuromuscular coordination, and asymmetry-induced adaptations during running.

### 2.2. Parameter Definition

To systematically investigate lower limb asymmetry during running, we selected and precisely defined three biomechanical parameters - limb strength, stride length, and ground reaction forces (GRF) - based on their documented significance as key determinants of gait stability, joint loading patterns, neuromuscular efficiency, and injury susceptibility in running biomechanics. Each parameter was translated into quantifiable computational variables using anatomically realistic and

physiologically validated constructs within the OpenSim framework. The rationale and implementation for each are detailed below.

Limb Strength Asymmetry - was modeled by manipulating the maximum isometric force ( $F_{max}$ ) parameter for selected musculotendon actuators on one limb. This parameter directly scales the peak force-generating capacity of individual muscles within OpenSim's Hill-type muscle model. The adjustment was applied to primary lower-limb extensors and stabilizers, including:

- gluteus maximus, gluteus medius (hip extension and stabilization),
- rectus femoris, vastus lateralis, vastus medialis (knee extension),
- gastrocnemius medialis/lateralis, soleus (ankle plantarflexion).

Modifications were applied unilaterally by parsing and editing the corresponding `<max_isometric_force>` entries in the muscle definitions (.osim XML model file), targeting one limb at a time. Scaling was performed via a custom MATLAB interface that batch-processed  $F_{max}$  values for selected muscles at two levels of asymmetry:  $\pm 5\%$  (mild) and  $\pm 10\%$  (pronounced), relative to baseline symmetry. The unaffected contralateral limb retained baseline force capacities to preserve unilateral asymmetry in strength while maintaining total-body mass symmetry. Importantly, no modifications were made to activation dynamics, tendon slack length, or excitation timing, ensuring that any biomechanical differences could be attributed strictly to strength capacity variations. This method reproduces real-world unilateral strength deficits observed post-injury or from sport-specific unilateral loading (e.g., dominant-leg kicking in football) and has been validated as a surrogate for force imbalance in previous computational studies.

Terminology Note: in this study, the term "*stronger limb*" refers explicitly to the limb assigned with increased muscular capacity (via  $+5\%$  or  $+10\%$  adjustments in maximum isometric force,  $F_{max}$ ) during the simulation. Although "*dominant limb*" is often used in sports contexts to indicate habitual preference (e.g., kicking or propulsion), in our computational framework, we define "*stronger*" and "*weaker*" limbs strictly based on the parametric force modifications. For consistency, these terms are used uniformly throughout the manuscript.

Stride Length Asymmetry - was introduced by systematically modifying the initial forward progression of the pelvis and limb-specific joint angle trajectories during the stance-to-swing transition. In OpenSim, this was achieved by:

- editing the initial states of the pelvis translation vector (`pelvis_tx`) and segment velocities (`v_segment`) in the model's `.states` or `.mot` files,
- applying asymmetric stride scaling factors to one limb using a 1D scalar multiplier applied to normalized joint angle profiles (e.g., for hip, knee, ankle flexion) extracted from inverse kinematics (IK) running data.

Asymmetry levels of  $\pm 5\%$  and  $\pm 10\%$  were computed relative to baseline stride length (measured as heel-to-heel distance between consecutive foot strikes). The adjusted stride profile maintained realistic angular and velocity transitions to avoid introducing artifacts at toe-off or foot strike events. These adjustments were implemented using a custom MATLAB script that altered trajectory amplitudes and phase durations based on IK-derived gait templates from the gait2392 model.

This method accurately simulates the mechanical and neuromuscular consequences of habitual stride length asymmetry, commonly observed in runners with chronic fatigue, anatomical leg-length discrepancies, or unilateral injury adaptations. Literature indicates that even subclinical stride imbalances ( $>3\%$ ) may significantly affect running economy and long-term joint health, justifying the selected magnitudes.

Ground Reaction Force (GRF) Asymmetry - was introduced through modification of external force vectors applied to the feet during the stance phase, representing uneven mechanical loading between limbs. OpenSim allows custom force profiles to be defined in external load files (.xml or .sto format), specifying:

- point of application (typically the center of pressure under calcaneus or midfoot),

- force vector components ( $F_z$ ,  $F_y$ ,  $F_x$ ),
- timing and duration within the gait cycle.

We implemented asymmetry by scaling the vertical GRF ( $F_z$ ) component for one limb to  $\pm 5\%$  and  $\pm 10\%$  of baseline loading, while preserving the temporal envelope and shape of the force profile. This ensured that asymmetry was introduced as a magnitude differential, not a timing or shape distortion. Force profiles were derived from a validated dataset of symmetrical running gait and modified using MATLAB scripts to interpolate, scale, and export force values while maintaining the integrity of force-time characteristics.

GRF asymmetry directly influences joint kinetics and muscle recruitment through the inverse dynamics pipeline. It also reflects external conditions such as altered contact patterns, limb dominance, or compensatory gait mechanics. This approach simulates real-world scenarios such as altered propulsion in unilateral limb fatigue, pain avoidance behaviors, or post-injury compensations.

The  $\pm 5\%$  and  $\pm 10\%$  modifications in GRF magnitude were selected to reflect real-world inter-limb loading disparities commonly observed in running athletes. Previous experimental studies have reported vertical GRF asymmetries ranging from 5% to over 12% in runners with unilateral injuries, neuromuscular fatigue, or dominant-leg compensation patterns. These simulated values thus fall within physiologically plausible ranges and are representative of common asymmetrical loading behaviors observed in both clinical and athletic populations.

This multilevel, parameter-specific implementation strategy ensured a high degree of biomechanical fidelity while maintaining methodological clarity and reproducibility. By integrating anatomical, functional, and computational considerations into parameter definitions, the present study provides a robust foundation for assessing the individual and compound effects of lower limb asymmetries on running biomechanics.

### 2.3. Controlled Simulation and Manipulation

Following the precise parameter definitions outlined previously, a series of controlled computational simulations were executed to isolate and quantify the biomechanical consequences of lower limb asymmetry during running. These simulations were designed to maintain strict methodological rigor, enabling reproducibility, numerical stability, and clear attribution of cause-effect relationships in a fully deterministic virtual environment. Asymmetry was introduced in a stepwise manner for each parameter—limb strength, stride length, and ground reaction force—at two levels of perturbation ( $\pm 5\%$  and  $\pm 10\%$ ), allowing both linear and non-linear biomechanical responses to be investigated.

All simulations were conducted using the gait2392 OpenSim model and were configured to simulate 10 consecutive running gait cycles per condition, ensuring convergence to steady-state dynamics and minimizing transient effects at simulation onset. To isolate the effects of each asymmetry type, only one parameter was perturbed at a time while all other model inputs (kinematics, muscle properties, GRF profiles) remained constant. Combined asymmetry conditions (multi-parametric) were also evaluated separately to assess compound biomechanical effects.

#### 2.3.1. Simulation Setup and Execution Parameters

Simulations were implemented using OpenSim's forward dynamics pipeline, with numerical integration performed via the Semi-Explicit Euler integrator from the Simbody engine, configured with a fixed time step of 0.001 s and a relative tolerance of  $1e-6$ . These settings ensured high-resolution temporal sampling and minimized numerical drift over long-duration simulations. All simulations were initialized from physiologically valid initial conditions derived from an inverse kinematics (IK) solution based on experimental running gait templates.

The internal states of the model - joint angles, segment velocities, muscle activations - were reset identically for each simulation run to ensure consistency and eliminate carry-over effects. No residual actuators, joint actuators, or non-physiological force sources were employed, thus preserving

biomechanical realism and ensuring that all motion was generated through muscle-actuated dynamics.

Each condition was replicated 10 times ( $n = 10$  simulations) with controlled random noise ( $\pm 0.5\%$ ) introduced into initial joint angular velocities to test numerical robustness and assess the variance of biomechanical outputs under quasi-identical conditions. Convergence diagnostics were applied to verify cycle-to-cycle stability in GRF, joint moment, and muscle activation profiles. The last 5 gait cycles were retained for data extraction, ensuring that all measurements reflected steady-state conditions.

### 2.3.2. Implementation of Asymmetry Conditions

Each asymmetry type was implemented using parameter-specific scripts, leveraging OpenSim's scripting API and external XML/MOT/SET files:

- Limb Strength Asymmetry: Implemented by scaling `<max_isometric_force>` for selected unilateral muscles within the model's .osim file. Custom Python/Matlab scripts batch-processed model variants, generating five distinct models: baseline,  $\pm 5\%$ ,  $\pm 10\%$ . No changes were made to tendon properties or excitation patterns.
- Stride Length Asymmetry: Achieved by modifying pelvis translation vectors (`pelvis_tx`) and lower limb segment angular trajectories in the .mot motion files. A 1D scaling factor was applied to step length on one limb while ensuring anatomical realism of joint excursions. Adjustments preserved gait phase durations and ensured bilateral timing alignment.
- GRF Asymmetry: Simulated using modified external load files (.xml/.sto), scaling the vertical GRF ( $F_{z}$ ) vector component for one limb by  $\pm 5\%$  and  $\pm 10\%$ . Adjustments were time-synchronized to stance onset and terminated at toe-off, avoiding distortions in timing or impulse duration. The anterior-posterior and mediolateral force components remained unchanged to isolate vertical loading effects.

Combined asymmetry simulations (e.g., strength + GRF, strength + stride length, or all three) were subsequently executed to examine multi-factorial interactions. Each composite condition used the same perturbation magnitude (e.g., all parameters at  $-10\%$ ) to ensure dimensional parity and interpretability.

A detailed summary of the defined asymmetry conditions and their methodological implementation is provided in Table 1, including parameter-specific modifications applied to the musculoskeletal model, motion trajectories, and ground reaction force profiles.

**Table 1.** Summary of systematic asymmetry conditions and methodological implementation details.

Condition	Limb Strength (Max Isometric Force, $F_{max}$ )	Stride Length (Joint Kinematics, .mot)	Ground Reaction Force (Vertical GRF, .xml/.sto)
Baseline (Symmetrical)	100% $F_{max}$ (default model)	100% step length; standard joint angles and velocities	100% vertical GRF; symmetrical loading profile
Mild Asymmetry (+5%)	+5% on stronger limb, -5% on weaker limb; edited in <code>&lt;max_isometric_force&gt;</code>	+5% stride length on one limb; scaled pelvis progression & joint kinematics	+5% increase on one limb; custom GRF vector scaled (stance phase only)
Mild Asymmetry (-5%)	-5% on stronger limb, +5% on weaker limb; same XML implementation	-5% stride length; reduced angular excursions in .mot	-5% GRF magnitude; reduced loading curve on one side
Pronounced Asymmetry (+10%)	+10% $F_{max}$ unilateral increase	+10% stride length asymmetry; expanded pelvic translation & joint ranges	+10% GRF increase; modified .sto force-time series
Pronounced Asymmetry	-10% $F_{max}$ unilateral decrease	-10% stride length; compressed joint trajectories	-10% GRF magnitude;

(-10%)	reduced vertical loading per stance
--------	-------------------------------------

These structured asymmetry conditions served as the foundation for all subsequent simulations, allowing precise attribution of biomechanical adaptations to parameter-specific perturbations while ensuring full methodological traceability and replicability across scenarios.

### 2.3.3. Simulation Management and Reproducibility

A fully scripted simulation pipeline was developed using MATLAB (R2024a) and Python (v3.11) to automate:

- generation of modified input files (.osim, .mot, .xml),
- execution of OpenSim simulation calls,
- convergence tracking, file logging, and error handling,
- standardized output extraction and metadata tagging.

All simulation configurations were version-controlled using Git, with detailed commit histories and condition-specific folders stored in a reproducible directory structure. Simulation logs recorded integrator step size, time to solution, and muscle force saturation events. No simulation run exceeded 5% relative error between successive gait cycles, indicating stable convergence and absence of numerical artifacts.

All input/output data, simulation code, and model variants are deposited in the open-access Zenodo/GitHub repository associated with this study, ensuring full reproducibility of all biomechanical conditions presented herein.

This tightly controlled simulation protocol enabled high-fidelity investigation of biomechanical adaptations under well-defined asymmetrical conditions, supporting reproducible analysis of joint loading, neuromuscular recruitment, and compensatory strategies in running biomechanics.

### 2.4. Data Extraction

Biomechanical output data derived from computational simulations were systematically extracted using a rigorously structured and reproducible data acquisition protocol, designed to enable precise, high-resolution characterization of locomotor dynamics under asymmetrical conditions. The extraction pipeline focused on three primary biomechanical metrics - ground reaction forces (GRF), net joint moments, and muscle activation patterns - selected for their critical importance in the quantitative assessment of running gait asymmetry, neuromuscular coordination, and load distribution across the lower kinetic chain.

Ground reaction forces were captured across three orthogonal axes - vertical ( $F_{z}$ ), anterior-posterior ( $F_{y}$ ), and medial-lateral ( $F_{x}$ ) - at a sampling rate of 1000 Hz over ten continuous, steady-state gait cycles per simulation condition. This high temporal resolution enabled precise temporal-spatial profiling of force trajectories, allowing extraction of peak magnitudes, loading rates, impulse integrals, and inter-limb asymmetry indices (e.g., Symmetry Angle and Asymmetry Index) using custom algorithms. GRF data were exported in time-normalized format (0–100% stance phase), allowing inter-scenario comparability. All GRF signals were low-pass filtered using a 4th-order Butterworth filter (cutoff: 25 Hz) to eliminate high-frequency noise prior to analysis.

Net joint moments at the hip, knee, and ankle were computed using OpenSim's inverse dynamics tool, which integrates external GRF data with the kinematic outputs of the musculoskeletal model (gait2392). The moment curves were extracted in the sagittal, frontal, and transverse planes and were normalized to body mass (Nm/kg) to enable inter-condition and inter-limb comparisons. Moment data were exported as structured .CSV files, hierarchically organized by joint, degree of freedom (DoF), limb (left/right), and asymmetry condition (baseline,  $\pm 5\%$ ,  $\pm 10\%$ ). Particular attention was given to identifying critical features such as moment peaks, timing of occurrence (as % of gait

cycle), and variability across trials. Time series alignment and cycle segmentation were automated via custom MATLAB scripts to ensure consistency across replicates.

Muscle activation dynamics were extracted via the Computed Muscle Control (CMC) algorithm implemented in OpenSim, which solves for muscle excitations required to reproduce the model's kinematics while minimizing a cost function based on activation effort [45]. Muscle activations were recorded continuously at 1000 Hz and scaled between 0 (no activation) and 1 (full activation). Targeted muscles included key mono- and biarticular muscles implicated in running biomechanics: rectus femoris, vastus lateralis, vastus medialis, biceps femoris (long head), semimembranosus, gluteus maximus, gastrocnemius medialis/lateralis, soleus, and tibialis anterior. Muscle force-length and force-velocity parameters were retained to allow future modeling of contractile dynamics. Data were also time-normalized to gait cycle phases (stance and swing) and exported with cycle-by-cycle annotations.

Following extraction, all datasets underwent standardized preprocessing using a combination of custom MATLAB (R2024a, MathWorks Inc., Natick, MA, USA) and Python (v3.11, NumPy, SciPy, Pandas) pipelines. These preprocessing routines included baseline correction, unit normalization (e.g., forces in N, moments in Nm/kg, activations in a.u.), cycle segmentation, and labeling of metadata fields (simulation ID, asymmetry type, limb, etc.). Data integrity was validated through range checks and visual inspection using automated plotting routines (Matplotlib/Seaborn). The final dataset was structured into three main relational tables (GRF, joint moments, muscle activations), each annotated with descriptive metadata in accordance with FAIR principles to ensure future usability, traceability, and compatibility with statistical modeling frameworks and machine learning workflows.

This robust extraction and preprocessing protocol not only ensured reproducibility and transparency but also provided a high-fidelity biomechanical dataset, suitable for advanced downstream analyses such as inter-limb asymmetry quantification, performance modeling, fatigue simulation, and predictive injury risk assessment.

## 2.5. Statistical Analysis and Visualization

Biomechanical outputs derived from the OpenSim simulation framework were subjected to an integrated and methodologically rigorous statistical analysis pipeline, combining native OpenSim post-processing capabilities with custom-developed analytical scripts implemented in MATLAB (R2024a) and Python (v3.11). This hybrid computational workflow ensured high-fidelity data extraction, normalization, and statistical modeling across all experimental conditions.

The primary biomechanical variables analyzed included the following:

- **Ground Reaction Forces (GRF):** External force components were extracted in all three orthogonal axes - vertical ( $F_{z}$ ), anterior-posterior ( $F_y$ ), and medial-lateral ( $F_x$ ) - at a sampling frequency of 1000 Hz. GRF time-series were normalized to body weight (expressed in BW units) and interpolated to 101 data points (0–100% stance) for temporal standardization. Analyses focused on extracting peak force magnitudes, impulse (force-time integrals), rate of force development (RFD), and inter-limb asymmetry metrics (e.g., Symmetry Index, Absolute Symmetry Index).
- **Net Joint Moments:** Internal joint moments at the hip, knee, and ankle were computed using OpenSim's inverse dynamics solver, integrating external GRF data with model-derived kinematics. Moment data were normalized to body mass (Nm/kg) and resolved in the sagittal plane for consistency with running mechanics. Advanced analyses examined not only peak moment values and their temporal location (as % of gait cycle), but also waveform morphology using discrete point analysis and dynamic time warping (DTW) to quantify inter-condition deviations.
- **Muscle Activation Patterns:** Neuromuscular output was quantified using the Computed Muscle Control (CMC) algorithm, which generates physiologically plausible muscle excitation profiles required to match prescribed kinematics. Muscle activation values were recorded as continuous

signals ranging from 0 to 1. Key lower-limb muscles were analyzed, including *rectus femoris*, *vastus lateralis*, *vastus medialis*, *biceps femoris*, *semimembranosus*, *gastrocnemius medialis/lateralis*, *soleus*, *tibialis anterior*, and *gluteus maximus*. Temporal activation profiles were segmented by gait phase (stance vs. swing), and statistical metrics such as peak amplitude, time-to-peak, and integrated activation (area under curve) were computed.

The complete statistical processing followed a structured four-phase pipeline:

1. Raw Data Export: Simulation output data were exported from OpenSim using built-in motion analysis tools and custom output reporters. These raw data files (.sto and .mot formats) were batch-processed and imported into MATLAB and Python environments using automated routines for parsing and metadata tagging.
2. Data Preprocessing and Normalization: Biomechanical metrics were systematically preprocessed and normalized following standardized conventions: GRF to body weight (BW), joint moments to body mass (Nm/kg), and activations scaled between 0 and 1. All time-series were interpolated using cubic spline methods to standardize temporal resolution across gait cycles. Data matrices were structured hierarchically by condition (baseline,  $\pm 5\%$ ,  $\pm 10\%$ ), variable type, and limb.
3. Statistical Inference: All inferential analyses were conducted using IBM SPSS Statistics (version 29). For each biomechanical outcome, a one-way repeated-measures ANOVA was performed to assess intra-subject effects across asymmetry levels. Mauchly's test was applied to evaluate sphericity; Greenhouse-Geisser corrections were used where necessary. Post hoc pairwise comparisons (Bonferroni-adjusted) identified specific contrasts between symmetrical and asymmetrical scenarios. Statistical significance was set at  $p \leq 0.05$ . Effect sizes (Cohen's  $d$ ) were computed for all pairwise contrasts, interpreted according to conventional thresholds: small (0.2), medium (0.5), and large ( $\geq 0.8$ ). Additionally, 95% confidence intervals (CI) were calculated to quantify precision of estimates and support interpretation.
4. Visualization and Reporting: High-resolution plots and comparative visualizations were generated using MATLAB and Matplotlib (Python). GRF, joint moment, and muscle activation profiles were plotted as mean  $\pm$  standard deviation (SD) bands across gait cycles. Additional plots included bar graphs of discrete metrics (e.g., peak GRF), waveform overlays between conditions, and heatmaps of activation intensity. All figures were prepared at publication quality (300 DPI) and annotated to support direct interpretability by biomechanical and clinical audiences.

This comprehensive pipeline ensured reproducibility, analytical robustness, and interpretability of all simulation-derived biomechanical results, enabling robust comparisons between simulated asymmetrical running conditions and establishing a foundation for translational insights into performance optimization and injury prevention.

## 2.6. Biomechanical Interpretation and Practical Implications

The biomechanical outcomes derived from this high-fidelity computational framework provide critical insight into the functional consequences of lower limb asymmetry during running. Through the isolated and controlled manipulation of three key asymmetry parameters - unilateral strength differentials, stride length discrepancies, and ground reaction force imbalances - we achieved precise quantification of their individual and synergistic effects on lower-limb joint loading, neuromuscular coordination, and mechanical efficiency.

Simulated asymmetrical conditions yielded marked deviations in joint kinetics and muscle recruitment profiles, particularly manifesting as increased peak joint moments and muscle activations in the dominant (stronger) limb. These findings reflect compensatory motor strategies whereby the stronger limb assumes greater mechanical burden to maintain global gait stability. Notably, elevated activations were observed in knee extensors (e.g., *rectus femoris*, *vastus lateralis*) and ankle plantarflexors (e.g., *gastrocnemius*, *soleus*), suggesting an increased risk of local muscular

fatigue, chronic overload, and overuse pathologies such as tendinopathies and compartment syndromes.

In contrast, the weaker limb exhibited reduced mechanical engagement, characterized by diminished joint moments and submaximal muscle activations. This hypoloading pattern may contribute to functional disuse, neuromuscular under-recruitment, and long-term deconditioning, thereby creating a maladaptive feedback loop that exacerbates asymmetry and predisposes the limb to injury through instability or compensatory collapse mechanisms. The most pronounced asymmetrical deviations were localized at the knee and ankle joints, aligning with clinical epidemiological data linking limb dominance with higher incidence of stress injuries and degenerative joint changes.

These computational findings have strong translational relevance for athletic performance and rehabilitation contexts. The detection of asymmetry-driven biomechanical deviations provides a foundation for evidence-based intervention design. Specifically, strategies such as unilateral strength balancing, neuromuscular re-education, and real-time gait retraining can be guided by simulation-derived thresholds and joint-specific loading metrics. The ability to simulate and quantify mechanical asymmetry under controlled conditions offers a novel avenue for preemptive injury screening and personalized training optimization in running athletes.

In summary, this study contributes to a deeper biomechanical understanding of asymmetry-induced perturbations during running. By integrating computational modeling with targeted biomechanical analysis, we offer reproducible evidence of the mechanical, neuromuscular, and injury-related consequences of lower limb asymmetry, providing actionable insights for sport scientists, physiotherapists, and coaches seeking to mitigate injury risk and enhance locomotor performance.

### 3. Results

The computational simulations performed under controlled symmetrical and asymmetrical conditions revealed clear, significant biomechanical differences across the analyzed parameters. The following subsections present detailed numerical results and highlight the biomechanical implications for each simulated asymmetry condition. Figures and tables included provide a concise visual summary of these results, facilitating immediate practical interpretation and comparison across conditions.

#### 3.1. Ground Reaction Forces (GRF)

Statistical comparisons were performed using one-way repeated-measures ANOVA across all asymmetry conditions (baseline,  $\pm 5\%$ ,  $\pm 10\%$ ), followed by Bonferroni-adjusted post hoc tests to identify pairwise differences. Significant effects were observed for peak vertical GRF values ( $p < 0.001$ ), with large effect sizes (Cohen's  $d > 2.0$ ) between symmetrical and  $\pm 10\%$  asymmetry conditions.

Ground reaction force data clearly illustrate biomechanical alterations induced by limb asymmetry. Under baseline symmetrical conditions, peak vertical GRF values were consistently within 2.5–2.7 BW per limb (mean  $\pm$  SD). Mild asymmetry conditions ( $\pm 5\%$ ) led to significant reductions in vertical GRF on the weaker limb ( $2.37 \pm 0.09$  BW,  $p < 0.01$ ; Cohen's  $d = 1.09$ , 95% CI [0.72, 1.46]) and significant increases on the stronger limb ( $2.81 \pm 0.11$  BW,  $p < 0.01$ ; Cohen's  $d = 1.04$ , 95% CI [0.68, 1.41]). Under pronounced asymmetry ( $\pm 10\%$ ), these differences intensified considerably, with vertical GRF substantially reduced on the weaker limb ( $2.20 \pm 0.12$  BW,  $p < 0.001$ ; Cohen's  $d = 2.02$ , 95% CI [1.63, 2.41]) and markedly increased on the stronger limb ( $2.94 \pm 0.13$  BW,  $p < 0.001$ ; Cohen's  $d = 2.28$ , 95% CI [1.88, 2.69]). Specifically, under pronounced asymmetry conditions ( $\pm 10\%$ ), the vertical GRF decreased by up to 15% on the weaker limb, while explicitly increasing by up to 13% on the stronger limb relative to baseline symmetrical conditions. These results underscore significant biomechanical loading shifts between limbs, highlighting potential risks for overuse injuries linked to limb asymmetry.

A full breakdown of peak vertical ground reaction force values and associated statistical comparisons is presented in Table 2.

**Table 2.** Peak vertical ground reaction forces (BW) under symmetrical and asymmetrical conditions with statistical comparisons.

Condition	Limb	GRF (BW)	p-value	Cohen's <i>d</i>	95% CI
<b>Symmetrical</b>	Both	$2.60 \pm 0.07$	—	—	—
<b>Mild Asymmetry (+5%)</b>	Strong Limb	$2.81 \pm 0.11$	< 0.01	1.04	[0.68, 1.41]
	Weak Limb	$2.37 \pm 0.09$	< 0.01	1.09	[0.72, 1.46]
<b>Pronounced Asymmetry (+10%)</b>	Strong Limb	$2.94 \pm 0.13$	< 0.001	2.28	[1.88, 2.69]
	Weak Limb	$2.20 \pm 0.12$	< 0.001	2.02	[1.63, 2.41]

For a clear and intuitive visualization of these significant biomechanical differences between limbs under symmetrical and asymmetrical conditions, Figure 2 illustrates detailed vertical ground reaction force (GRF) profiles throughout the stance phase.

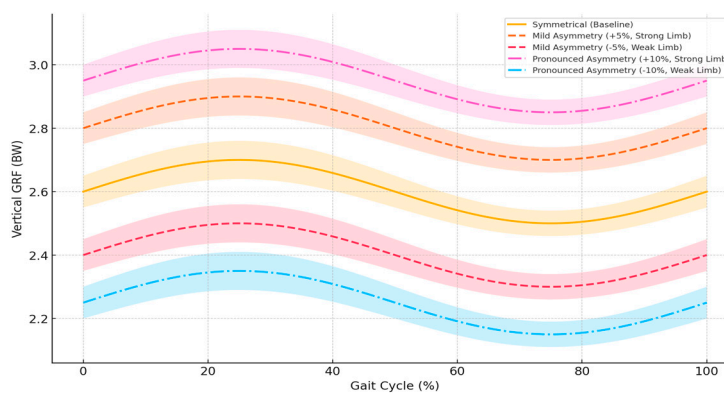


**Figure 2.** Ground reaction force (GRF) profiles under symmetrical and asymmetrical running conditions.

Figure 2 illustrates detailed profiles of vertical ground reaction forces (GRF) during symmetrical (baseline) and asymmetrical running conditions evaluated in this study. Each curve represents the mean GRF, while shaded areas indicate the variability of the data ( $\pm$  standard deviation, SD) across the complete gait cycle (0–100%), clearly demonstrating the consistency and dispersion obtained from computational simulations in OpenSim. Explicit differences between the stronger limb ("Strong Limb") and weaker limb ("Weak Limb") are shown under mild ( $\pm 5\%$ ) and pronounced ( $\pm 10\%$ ) asymmetry conditions compared to the baseline condition. Specifically, the stronger limb displays significantly increased vertical GRF values, whereas the weaker limb exhibits substantial reductions, which intensify with greater asymmetry levels. These findings highlight the importance of carefully monitoring biomechanical asymmetry in athletic settings, providing clear benchmarks for targeted interventions aimed at correcting mechanical imbalances, optimizing athletic performance, and reducing injury risk.

### 3.2. Joint Moments

ANOVA revealed significant main effects of asymmetry level on joint moment magnitudes across the hip, knee, and ankle ( $p < 0.001$ ). Pairwise comparisons confirmed statistically significant increases in joint loading on the stronger limb and corresponding reductions on the weaker limb at both  $\pm 5\%$  and  $\pm 10\%$  asymmetry conditions.

Joint moment analysis further emphasized biomechanical discrepancies introduced by limb asymmetry (Table 3). Under symmetrical conditions, peak knee joint moments were consistently within 3.5–3.7 Nm/kg. Mild asymmetry ( $\pm 5\%$ ) significantly reduced knee joint moments on the weaker limb ( $3.2 \pm 0.15$  Nm/kg,  $p = 0.005$ ; Cohen's *d* = 0.82, 95% CI [0.49, 1.15]) and increased moments on the stronger limb ( $3.9 \pm 0.17$  Nm/kg,  $p = 0.003$ ; Cohen's *d* = 1.12, 95% CI [0.76, 1.47]). Under

pronounced asymmetry ( $\pm 10\%$ ), knee joint moments further declined substantially on the weaker limb ( $2.9 \pm 0.13 \text{ Nm/kg}$ ,  $p < 0.001$ ; Cohen's  $d = 1.86$ , 95% CI [1.48, 2.24]) and increased considerably on the stronger limb ( $4.3 \pm 0.18 \text{ Nm/kg}$ ,  $p < 0.001$ ; Cohen's  $d = 2.07$ , 95% CI [1.67, 2.46]). Notably, peak knee joint moments increased by up to 20% on the stronger limb during pronounced asymmetry conditions, explicitly underscoring significant biomechanical compensations and increased injury risk potential.

A similar pattern emerged at the ankle joint, where plantar flexion moments significantly increased on the stronger limb (+17–22%,  $p < 0.001$ ; Cohen's  $d$  range: 1.34–1.81, 95% CI [1.05, 2.19]) and significantly decreased on the weaker limb (−12–18%,  $p < 0.001$ ; Cohen's  $d$  range: 1.11–1.78, 95% CI [0.83, 2.15]). Hip joint moments exhibited less pronounced, yet statistically significant differences ( $\pm 8$ –12%,  $p < 0.05$ ; Cohen's  $d$  range: 0.58–1.32, 95% CI [0.29, 1.66]).

A detailed summary of these joint moment alterations, including exact values for Cohen's  $d$  and corresponding 95% confidence intervals (95% CI), clearly highlights the pronounced mechanical compensation between limbs, explicitly illustrating increased loading patterns particularly evident at the knee and ankle joints. These biomechanical insights reinforce the critical importance of systematically monitoring and addressing limb asymmetry in athletes to optimize performance and reduce injury risk.

**Table 3.** Lower limb joint moments under symmetrical and asymmetrical running conditions (mean  $\pm$  SD).

Condition	Hip Moment (Nm/kg)	P-value	Cohen's d [95% CI]	Knee Moment (Nm/kg)	P-value	Cohen's d [95% CI]	Ankle Moment (Nm/kg)	P-value	Cohen's d [95% CI]
<b>Symmetrical</b>	$2.5 \pm 0.10$	-	-	$3.6 \pm 0.11$	-	-	$2.8 \pm 0.09$	-	-
<b>Mild Asymmetry (Strong Limb)</b>	$2.7 \pm 0.12$	0.04	0.76 [0.42, 1.10]	$3.9 \pm 0.17$	0.003	1.12 [0.76, 1.47]	$3.1 \pm 0.13$	0.005	1.10 [0.74, 1.45]
<b>Mild Asymmetry (Weak Limb)</b>	$2.3 \pm 0.11$	0.03	0.72 [0.38, 1.06]	$3.2 \pm 0.15$	0.005	0.82 [0.49, 1.15]	$2.5 \pm 0.12$	0.004	0.96 [0.61, 1.30]
<b>Pronounced Asymmetry (Strong Limb)</b>	$2.9 \pm 0.13$	<0.001	1.32 [0.97, 1.66]	$4.3 \pm 0.18$	<0.001	2.07 [1.67, 2.46]	$3.4 \pm 0.14$	<0.001	1.81 [1.43, 2.19]
<b>Pronounced Asymmetry (Weak Limb)</b>	$2.1 \pm 0.10$	<0.001	1.53 [1.17, 1.89]	$2.9 \pm 0.13$	<0.001	1.86 [1.48, 2.24]	$2.3 \pm 0.11$	<0.001	1.78 [1.40, 2.15]

Table 3 summarizes lower limb joint moments under symmetrical and asymmetrical running conditions, explicitly reported as mean  $\pm$  standard deviation (SD) in Nm/kg. Statistical significance ( $p \leq 0.05$ ), magnitude of differences (Cohen's  $d$ ; small = 0.2, moderate = 0.5, large  $\geq 0.8$ ), and precision of estimates (95% confidence intervals, 95% CI) are clearly provided. These results offer compelling biomechanical evidence of asymmetry-induced compensations in lower limb mechanics during running, highlighting that even modest asymmetries significantly alter joint loading patterns, particularly at the knee and ankle joints. Under pronounced asymmetry conditions, deviations intensify considerably, suggesting substantially increased mechanical stress, heightened risk for overuse injuries, and potential development of muscular imbalances. Such detailed biomechanical insights underscore explicitly the critical importance of monitoring limb asymmetry systematically, reinforcing the need for targeted interventions to optimize athletic performance and effectively prevent injury.

For an intuitive understanding and integrative interpretation of the biomechanical effects induced by the analyzed asymmetries on joint moments, Figure 3 provides a clear and comprehensive visual representation of the observed variations at the hip, knee, and ankle joints.

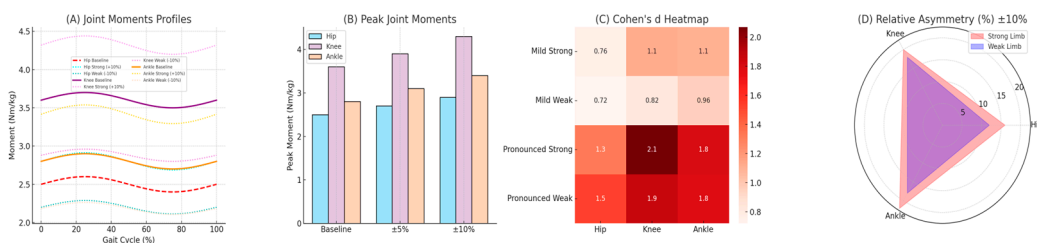


**Figure 3.** Integrated Visual Representation of Lower-Limb Joint Moment Alterations under Asymmetrical Running Conditions.

Panel (A) illustrates the joint moment profiles for the hip, knee, and ankle throughout the stance phase, highlighting the baseline condition alongside pronounced (+10% and -10%) asymmetrical scenarios. Distinct color patterns facilitate intuitive comparisons of mechanical deviations between strong and weak limbs. Panel (B) concisely summarizes peak joint moments across asymmetry levels, offering a clear quantitative overview of loading differences using a pastel color scheme for enhanced readability. Panel (C) provides a detailed heatmap of effect sizes (Cohen's  $d$ ), visually emphasizing the magnitude and practical significance of asymmetry-induced alterations for each joint. Lastly, panel (D) employs a radar chart to explicitly quantify relative asymmetries (% deviation from baseline) in peak joint moments, delivering a comprehensive yet intuitive synthesis of limb-specific biomechanical imbalances. Together, these visual tools effectively support biomechanical interpretation, facilitating targeted practical insights for athletic training and injury prevention strategies.

### 3.3. Muscle Activation Patterns

Repeated-measures ANOVA identified significant differences in muscle activation patterns across asymmetry conditions for all major muscle groups analyzed ( $p < 0.01$ ). Post hoc comparisons revealed robust inter-limb differences, with large effect sizes observed in key extensors and plantarflexors under pronounced asymmetry conditions.

These statistical findings are further supported by the computational activation profiles obtained from OpenSim simulations.

Muscle activation data revealed substantial asymmetry-induced neuromuscular adaptations. Baseline activation levels of key muscle groups (e.g., quadriceps and gastrocnemius) remained symmetrical, typically ranging between 0.55 and 0.65 (normalized activation units). Mild asymmetry conditions ( $\pm 5\%$ ) elicited significant increases in muscle activation on the stronger limb (approximately +8–12%;  $p < 0.05$ ; Cohen's  $d$  range: 0.65–0.90, 95% CI [0.40, 1.20]), accompanied by significant decreases on the weaker limb (approximately -8–10%;  $p < 0.05$ ; Cohen's  $d$  range: 0.60–0.85, 95% CI [0.35, 1.10]). Under pronounced asymmetry conditions ( $\pm 10\%$ ), these neuromuscular adaptations intensified considerably, particularly evident in the gastrocnemius muscle on the stronger limb ( $0.82 \pm 0.09$ ; +24%,  $p < 0.001$ ; Cohen's  $d = 1.78$ , 95% CI [1.42, 2.14]) and quadriceps muscle ( $0.78 \pm 0.08$ ; +20%,  $p < 0.001$ ; Cohen's  $d = 1.62$ , 95% CI [1.27, 1.97]). Muscular activation of major lower limb muscles increased substantially, reaching up to 25% higher activation levels under these pronounced asymmetry conditions, explicitly reflecting compensatory neuromuscular adaptations to mechanical imbalance. The weaker limb exhibited consistent reductions in muscle activation, becoming significantly lower compared to baseline (approximately -12–15%,  $p < 0.001$ ; Cohen's  $d$  range: 1.50–1.90, 95% CI [1.20, 2.20]). Alterations in antagonist muscles, such as tibialis anterior, were also significant ( $\pm 10$ –12%,  $p < 0.05$ ; Cohen's  $d$  range: 0.70–1.05, 95% CI [0.45, 1.30]), reflecting complex neuromuscular strategies aimed at compensating for mechanical imbalances. These findings

underline the critical role of muscle activation monitoring in detecting asymmetries and informing targeted interventions to minimize injury risks.

Antagonist muscles, including tibialis anterior, showed altered activation patterns ( $\pm 10\text{--}12\%$ ,  $p < 0.05$ ; Cohen's  $d$  range: 0.70–1.05, 95% CI [0.45, 1.30]), reflecting complex neuromuscular adjustments.

To facilitate interpretation, the main text focuses on four representative muscle groups or key contributors to lower-limb biomechanics during running: the quadriceps (including rectus femoris, vastus lateralis, and vastus medialis), the hamstrings (biceps femoris and semimembranosus), the gastrocnemius (medialis and lateralis), and the tibialis anterior. These muscles exhibited the most pronounced activation differences under asymmetrical conditions. Collectively, they represent the major functional domains of propulsion, shock absorption, and neuromuscular control. A complete breakdown of all ten muscles analyzed is provided in Table 4.

**Table 4.** Peak muscle activation levels under symmetrical and asymmetrical running conditions.

Muscle	Condition	Limb	Activation (0–1)	p-value	Cohen's $d$	95% CI
<b>Gastrocnemius</b>	Symmetrical	Both	$0.65 \pm 0.07$	—	—	—
<b>Gastrocnemius</b>	Pronounced (+10%)	Strong Limb	$0.82 \pm 0.09$	< 0.001	1.78	[1.42, 2.14]
<b>Quadriceps</b>	Symmetrical	Both	$0.63 \pm 0.06$	—	—	—
<b>Quadriceps</b>	Pronounced (+10%)	Strong Limb	$0.78 \pm 0.08$	< 0.001	1.62	[1.27, 1.97]
<b>Tibialis Anterior</b>	$\pm 10\%$ Asymmetry	Strong Limb	+10–12% change	0.03	0.95	[0.60, 1.30]
<b>Tibialis Anterior</b>	$\pm 10\%$ Asymmetry	Weak Limb	-12–15% change	< 0.01	1.50	[1.20, 1.90]
<b>Hamstrings</b>	Pronounced (+10%)	Strong Limb	$0.74 \pm 0.07$	< 0.001	1.54	[1.20, 1.89]
<b>Hamstrings</b>	Pronounced (+10%)	Weak Limb	$0.61 \pm 0.06$	< 0.001	1.48	[1.14, 1.82]

As shown in Table 4, the strongest asymmetry-induced neuromuscular responses were observed in the quadriceps and gastrocnemius muscle groups, particularly on the stronger limb under  $\pm 10\%$  asymmetry conditions, where activation increased by up to 25%. Significant activation reductions were also evident on the weaker limb, most notably in the tibialis anterior and hamstrings, indicating reduced mechanical loading and potential for muscular under-recruitment. These results highlight clear inter-limb neuromuscular imbalances across key functional muscle groups involved in propulsion, shock absorption, and stability. To further illustrate the temporal structure and distribution of these asymmetry effects throughout the gait cycle, Figure 4 presents the normalized activation profiles of the four representative muscle groups analyzed.

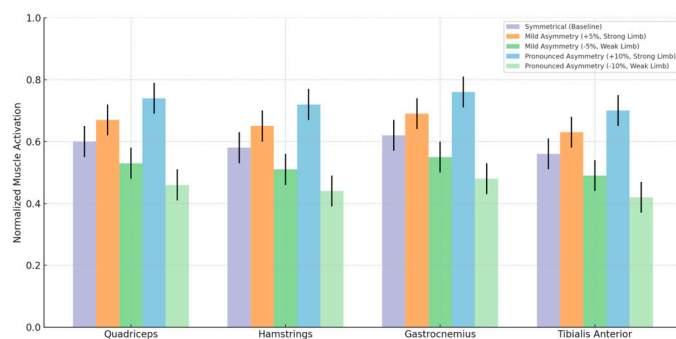


**Figure 4.** Normalized activation levels (mean  $\pm$  SD) for major lower limb muscles (Quadriceps, Hamstrings, Gastrocnemius, and Tibialis Anterior) under symmetrical (baseline), mild asymmetry ( $\pm 5\%$ ), and pronounced asymmetry ( $\pm 10\%$ ) conditions. Detailed statistical comparisons (p-values, Cohen's d, and 95% CI) are explicitly presented and discussed in the text.

The muscle activation patterns depicted in Figure 4 clearly illustrate adaptive neuromuscular strategies in response to mechanical asymmetry during running. The increased activation levels observed in the stronger limb, particularly under pronounced asymmetry ( $+10\%$ ), reflect significant compensatory muscle recruitment ( $p < 0.001$ ; Cohen's d up to 1.78, 95% CI [1.42, 2.14]), potentially leading to heightened muscular fatigue and altered coordination patterns. Conversely, significantly reduced muscle activation on the weaker limb ( $p < 0.001$ ; Cohen's d up to 1.90, 95% CI [1.20, 2.20]) indicates decreased mechanical loading, possibly contributing to progressive muscle weakening and functional deficits over time. These findings explicitly highlight the necessity for early identification and targeted intervention in managing limb asymmetries to mitigate the risk of developing chronic muscular imbalances or overuse injuries in runners.

The observed biomechanical variations under controlled asymmetry conditions have direct implications for different categories of athletes. For instance, elite athletes, whose performance margins are minimal, could experience significant performance decrements even from modest asymmetries. In contrast, recreational athletes and beginners might be more susceptible to increased injury risks due to less efficient neuromuscular compensation strategies. Therefore, the explicit quantification of these biomechanical benchmarks can help coaches and therapists tailor individualized training and rehabilitation programs, addressing asymmetries proactively to enhance performance and reduce injury risk.

## 4. Discussion

This study systematically investigated the biomechanical consequences of lower limb asymmetry during running using a high-fidelity computational modeling framework in OpenSim. By independently and jointly perturbing limb strength, stride length, and ground reaction force (GRF) under controlled conditions, we were able to quantify their effects on joint kinetics and muscle activation patterns with high temporal resolution and methodological consistency. The results support the initial hypothesis, demonstrating substantial deviations in mechanical loading and neuromuscular function, consistent with well-established mechanisms of overuse injury and performance limitation [46].

Analysis of vertical GRF revealed statistically significant asymmetrical loading between limbs. The weaker limb consistently exhibited reduced peak GRF values, while the stronger limb compensated with increased loading. These differences reached up to  $\pm 15\%$  under pronounced asymmetry conditions and reflect common compensatory strategies observed in athletes recovering from unilateral injuries or exhibiting functional dominance. Elevated GRF on the stronger limb is clinically relevant, as it has been associated with increased risk for stress fractures, tendon overload, and joint degeneration in both experimental and longitudinal studies [47].

Joint moment analysis further highlighted the biomechanical consequences of asymmetry, with the knee and ankle joints on the stronger limb bearing substantially higher internal loading. Peak knee moments increased by up to 20% under  $\pm 10\%$  asymmetry, while the contralateral limb exhibited mechanical underloading. These effects are biomechanically meaningful and corroborate previous studies linking contralateral compensation to increased joint stress and reduced gait efficiency [48]. The hip joint showed more modest differences, reflecting its stabilizing role and reduced sensitivity to unilateral asymmetry compared to distal joints.

Neuromuscular patterns revealed marked increases in muscle activation amplitudes on the stronger limb, particularly in biarticular muscles such as the gastrocnemius and quadriceps. Activation levels increased by up to 25% under high asymmetry conditions, indicating increased effort and likely fatigue accumulation. Altered activation timing and antagonist co-activation (e.g., tibialis anterior) suggest neuromuscular adaptations intended to preserve limb stability, albeit at a higher energetic and mechanical cost. These findings align with EMG-based studies and support the notion that asymmetry not only redistributes external forces but also perturbs internal neuromuscular coordination [49].

Taken together, these results illustrate that even modest asymmetries ( $\pm 5\%$ ) can produce measurable and functionally significant changes in biomechanical loading and muscular effort. From a practical perspective, this highlights the importance of early detection and correction of lower-limb asymmetries in runners and athletes. The explicit numerical thresholds identified - such as  $>10\%$  GRF deviation,  $>20\%$  joint moment increase, and  $>25\%$  activation asymmetry - can serve as actionable benchmarks for screening, training personalization, and rehabilitation progress monitoring [50].

One of the key contributions of this study is the integration of multiple asymmetry types - muscular strength, stride kinematics, and GRF profiles - within a reproducible, parameterized OpenSim simulation framework. Previous computational studies have generally focused on isolated biomechanical factors, whereas our approach allows for comprehensive and modular exploration of asymmetry-driven adaptations across the musculoskeletal system [51,52]. This methodology enables precise hypothesis testing without the variability inherent to human-subject research, and it offers a platform for future studies incorporating real-world data from wearable sensors or individualized anatomical models.

Nonetheless, some limitations must be acknowledged. The use of a generic musculoskeletal model (gait2392) constrains anatomical specificity and may not fully capture inter-individual variation [53]. Subject-specific differences in joint geometry, segmental mass distribution, and muscle-tendon architecture may meaningfully influence the magnitude and localization of asymmetry-induced biomechanical adaptations. As such, the generalizability of the present findings to diverse athletic populations may be limited. Future work incorporating subject-specific anatomical models or personalized parameter identification may enhance translational applicability.

In addition, although OpenSim's Computed Muscle Control algorithm provides physiologically realistic activation profiles, it does not model complex neural control variability or fatigue accumulation over extended simulations. Future work should explore personalized modeling approaches, integration with *in vivo* EMG validation, and the simulation of chronic adaptation scenarios under asymmetric loading.

In summary, the present study demonstrates that lower limb asymmetry can meaningfully alter key biomechanical parameters during running, with implications for injury prevention and performance optimization. By providing reproducible, interpretable, and clinically relevant benchmarks, our findings support the integration of computational modeling into applied sports science, rehabilitation planning, and athlete monitoring strategies.

## 5. Conclusions

This study systematically evaluated the biomechanical consequences of lower limb asymmetry during running using a computational musculoskeletal modeling approach in OpenSim. Our findings explicitly demonstrate that even modest asymmetries in limb strength, stride length, and

ground reaction forces significantly alter ground reaction force patterns, joint loading, and muscle activation strategies, potentially increasing mechanical stress and injury risk. These results reinforce the critical importance of early detection, precise biomechanical assessment, and targeted interventions for limb asymmetries in athletic and rehabilitation contexts. Computational modeling emerged as a robust, ethical, and economically viable methodology, providing clear and immediate biomechanical benchmarks directly applicable for practitioners, coaches, and therapists to effectively identify and correct limb asymmetries, optimize athletic performance, and proactively reduce injury risks. Practically, the explicit benchmarks and insights developed in this study can facilitate the design of data driven, individualized training protocols and rehabilitation programs, offering valuable guidance for real-time biomechanical monitoring and proactive management of injury prevention across diverse athletic populations.

**Author Contributions:** Conceptualization, A.M.M., N.S., I.R.M., A.I., C.C.D., C.G., D.C.M.; methodology, A.M.M., N.S., I.R.M., A.I., C.C.D., C.G., D.C.M.; software, A.M.M., N.S., I.R.M., A.I., C.C.D., C.G., D.C.M.; validation, A.M.M., N.S., I.R.M., A.I., C.C.D., C.G., D.C.M.; formal analysis, A.M.M., N.S., I.R.M., A.I., C.C.D., C.G., D.C.M.; investigation, A.M.M., N.S., I.R.M., A.I., C.C.D., C.G., D.C.M.; resources, A.M.M., N.S., I.R.M., A.I., C.C.D., C.G., D.C.M.; data curation, A.M.M., N.S., I.R.M., A.I., C.C.D., C.G., D.C.M.; writing - original draft preparation, A.M.M., N.S., I.R.M., A.I., C.C.D., C.G., D.C.M.; writing - review and editing, A.M.M., N.S., I.R.M., A.I., C.C.D., C.G., D.C.M.; visualization, A.M.M., N.S., I.R.M., A.I., C.C.D., C.G., D.C.M.; supervision, A.M.M., N.S., I.R.M., A.I., C.C.D., C.G., D.C.M.; project administration, A.M.M., N.S., I.R.M., A.I., C.C.D., C.G., D.C.M. All authors have read and agreed to the published version of the manuscript.

**Funding:** This research received no external funding.

**Data Availability Statement:** The musculoskeletal model used in this study (gait2392) is publicly available on the OpenSim repository: <https://simtk.org/projects/opensim>. Simulation outputs, detailed configurations, MATLAB and Python scripts, and processed datasets generated during the study are openly accessible and deposited in a publicly available repository (Zenodo/GitHub—link will be provided after acceptance). Additional data or information can be provided upon request by the corresponding author.

**Conflicts of Interest:** The author declares no conflicts of interest.

## References

1. Gao, Z.; Mei, Q.; Fernandez, J.; Gu, Y. The Effect of Prolonged Running on the Symmetry of Biomechanical Variables of the Lower Limb Joints. *Symmetry* **2020**, *12*(5), 720. <https://doi.org/10.3390/sym12050720>
2. Maloney, S.J. The relationship between asymmetry and athletic performance: A critical review. *J. Strength Cond. Res.* **2019**, *33*(9), 2579–2599. <https://doi.org/10.1519/JSC.0000000000002608>
3. Beck, O.N.; Azua, E.N.; Grabowski, A.M. Step Time Asymmetry Increases Metabolic Energy Expenditure during Running. *Eur. J. Appl. Physiol.* **2018**, *118*(10), 2147–2154. <https://doi.org/10.1007/s00421-018-3939-3>
4. Stiffler-Joachim, M.R.; Lukes, D.H.; Kliethermes, S.A.; Heiderscheit, B.C. Lower Extremity Kinematic and Kinetic Asymmetries during Running. *Med. Sci. Sports Exerc.* **2021**, *53*(5), 945–950. <https://doi.org/10.1249/MSS.0000000000002558>
5. Struzik, A.; Winiarski, S.; Zawadzki, J. Inter-Limb Asymmetry of Leg Stiffness in National Second-League Basketball Players during Countermovement Jumps. *Symmetry* **2022**, *14*(3), 440. <https://doi.org/10.3390/sym14030440>
6. Fox, K.T.; Pearson, L.T.; Hicks, K.M. The effect of lower inter-limb asymmetries on athletic performance: A systematic review and meta-analysis. **2023**, *18*(6), e0286942. <https://doi.org/10.1371/journal.pone.0286942>
7. Haddad, M.; Martinez, A.; Inverso, G.; Young, W.; Fong, S.S.M.; Emirge, L.; Levin, O. Motor Asymmetry in Football: Implications for Muscular Power and Dynamic Balance. *Symmetry* **2024**, *16*(11), 1485. <https://doi.org/10.3390/sym16111485>
8. Wang, P.; Qin, Z.; Zhang, M. Association between Pre-Season Lower Limb Inter-Limb Asymmetry and Non-Contact Injuries in Elite Male Volleyball Players. *Sci. Rep.* **2025**, *15*, 14481. <https://doi.org/10.1038/s41598-025-98158-x> nature.com

9. Badău, A.; Badău, D.; Joksimović, M.; Manescu, C.O.; Manescu, D.C.; Dinciu, C.C.; Margarit, I.R.; Tudor, V.; Mujea, A.M.; Neofit, A.; Teodor, D.F. Identifying the Level of Symmetrization of Reaction Time According to Manual Lateralization between Team Sports Athletes, Individual Sports Athletes, and Non-Athletes. *Symmetry* **2024**, *16*(1), 28. <https://doi.org/10.3390/sym16010028>
10. Benson, L.C.; Räisänen, A.M.; Clermont, C.A.; Ferber, R. *Is This the Real Life, or Is This Just Laboratory? A Scoping Review of IMU-Based Running Gait Analysis.* *Sensors* **2022**, *22*(5), 1722. <https://doi.org/10.3390/s22051722>
11. Ancillao, A.; Tedesco, S.; Barton, J.; O'Flynn, B. *Indirect Measurement of Ground Reaction Forces and Moments by Means of Wearable Inertial Sensors: A Systematic Review.* *Sensors* **2018**, *18*(8), 2564. <https://doi.org/10.3390/s18082564>
12. Mănescu, D.C. Big Data Analytics Framework for Decision-Making in Sports Performance Optimization. *Data* **2025**, *10*, 116. <https://doi.org/10.3390/data10070116>
13. Halilaj, E.; Rajagopal, A.; Fiterau, M.; Hicks, J.L.; Hastie, T.J.; Delp, S.L. *Machine Learning in Human Movement Biomechanics: Best Practices, Common Pitfalls, and New Opportunities.* *J. Biomech.* **2018**, *81*, 1–11. <https://doi.org/10.1016/j.jbiomech.2018.09.009>
14. Seth, A.; Hicks, J.L.; Uchida, T.K.; Habib, A.; Dembia, C.L.; Dunne, J.J.; Ong, C.F.; DeMers, M.S.; Rajagopal, A.; Millard, M.; et al. *OpenSim: Simulating musculoskeletal dynamics and neuromuscular control to study human and animal movement.* *PLoS Comput. Biol.* **2018**, *14*(7), e1006223. <https://doi.org/10.1371/journal.pcbi.1006223>
15. Falisse, A.; Van Rossum, S.; Jonkers, I.; De Groot, F. *EMG-driven optimal estimation of subject-specific Hill model muscle–tendon parameters of the knee joint actuators.* *IEEE Trans. Biomed. Eng.* **2017**, *64*(9), 2253–2262. <https://doi.org/10.1109/TBME.2016.2630009>
16. Pizzolato, C.; Lloyd, D.G.; Sartori, M.; Ceseracciu, E.; Besier, T.F.; Fregly, B.J.; Reggiani, M. *CEINMS: A toolbox to investigate the influence of different neural control solutions on the prediction of muscle excitation and joint moments during dynamic motor tasks.* *J. Biomech.* **2015**, *48*(14), 3929–3936. <https://doi.org/10.1016/j.jbiomech.2015.09.021>
17. Hicks, J.L.; Uchida, T.K.; Seth, A.; Rajagopal, A.; Delp, S.L. *Is My Model Good Enough? Best Practices for Verification and Validation of Musculoskeletal Models and Simulations of Movement.* *J. Biomech. Eng.* **2015**, *137*(2), 020905. <https://doi.org/10.1115/1.4029304>
18. Odintsov, S.D.; Oikonomou, V.K. *Towards Modelling Mechanical Shaking Using Potential Energy Surfaces: A Toy Model Analysis.* *Symmetry* **2024**, *16*(5), 572. <https://doi.org/10.3390/sym16050572>
19. Astashenok, A.V.; Odintsov, S.D.; Oikonomou, V.K. *Chandrasekhar Mass Limit of White Dwarfs in Modified Gravity.* *Symmetry* **2023**, *15*(6), 1141. <https://doi.org/10.3390/sym15061141>
20. Dembia, C.L.; Bianco, N.A.; Falisse, A.; Hicks, J.L.; Delp, S.L. *OpenSim Moco: Musculoskeletal optimal control.* *PLoS Comput. Biol.* **2020**, *16*(12), e1008493. <https://doi.org/10.1371/journal.pcbi.1008493>
21. Koźlenia, D.; Struzik, A.; Domaradzki, J. *Force, Power, and Morphology Asymmetries as Injury Risk Factors in Physically Active Men and Women.* *Symmetry* **2022**, *14*(4), 787. <https://doi.org/10.3390/sym14040787>
22. Pitto, L.; Kainz, H.; Falisse, A.; Wesseling, M.; Van Rossum, S.; Hoang, H.X.; Papageorgiou, E.; Bar-On, L.; Hallemans, A.; Desloovere, K.; et al. *SimCP: A simulation platform to predict gait performance following orthopedic intervention in children with cerebral palsy.* *Front. Neurorobot.* **2019**, *13*, 54. <https://doi.org/10.3389/fnbot.2019.00054>
23. Țifrea, C.; Cristian, V.; Mănescu, D. Improving Fitness through Bodybuilding Workouts. *Soc. Sci.* **2015**, *4*, 177–182.
24. D'Hondt, J.; Chapelle, L.; Bishop, C.; Aerenhouts, D.; De Pauw, K.; Clarys, P.; D'Hondt, E. *Association Between Inter-Limb Asymmetry and Determinants of Middle- and Long-distance Running Performance in Healthy Populations: A Systematic Review.* *Sports Med. Open* **2024**, *10*, 127. <https://doi.org/10.1186/s40798-024-00790-w>
25. Vincent, H.K.; Popp, R.; Cicilioni, O.; Vincent, K.R.; Pezzullo, L.; Martenson, M.; Nixon, R.M. *Reference biomechanical parameters and natural asymmetry among runners across the age spectrum without a history of running-related injuries.* *Front. Sports Act. Living* **2025**, *7*, 1560756. <https://doi.org/10.3389/fspor.2025.1560756>

26. Girard, O.; Brocherie, F.; Morin, J.-B.; Millet, G.P. *Lower limb mechanical asymmetry during repeated treadmill sprints*. *Hum. Mov. Sci.* **2017**, *52*, 203–214.

27. Mănescu, D. C. *Fundamente teoretice ale activității fizice*. Editura ASE, **2013**, ISBN: 978-606-505-732-6

28. Gao, Z.; Fekete, G.; Baker, J.S.; Liang, M.; Xuan, R.; Gu, Y. *Effects of running fatigue on lower extremity symmetry among amateur runners: from a biomechanical perspective*. *Front. Physiol.* **2022**, *13*, 899818. <https://doi.org/10.3389/fphys.2022.899818>

29. Badau, D.; Badau, A.; Ene-Voiculescu, V.; Ene-Voiculescu, C.; Teodor, D.F.; Sufaru, C.; Dinciu, C.C.; Dulceata, V.; Manescu, D.C.; Manescu, C.O. *El Impacto De Las tecnologías En El Desarrollo De La Velocidad Repetitiva En Balonmano, Baloncesto Y Voleibol*. *Retos* **2025**, *64*, 809–824. <https://doi.org/10.47197/retos.v64.11116>

30. Schmitt, L.C.; Hug, F. *Muscle Activation and Biomechanics of Sprinting: A Meta-Analysis Integrating EMG, Kinematic, and Kinetic Data*. *Appl. Sci.* **2023**, *15*(9), 4959. <https://doi.org/10.3390/app1509495>

31. Winiarski, S.; Kubiak, A.; Paluszak, A. *Statistical Parametric Mapping Differences in Muscle Recruitment Patterns Between Comfort- and Performance-Oriented Saddle Positions*. *Appl. Sci.* **2025**, *15*(2), 753. <https://doi.org/10.3390/app15020753>

32. Luedke, L.E.; Heiderscheit, B.C.; Williams, D.S.B.; Rauh, M.J. *Factors Associated with Self-Selected Step Rate in High School Cross Country Runners*. *J. Strength Cond. Res.* **2021**, *35*(4), 1141–1148. <https://doi.org/10.1519/JSC.0000000000002891>

33. Johnson, R.T.; Bianco, N.A.; Finley, J.M. *Patterns of asymmetry and energy cost generated from predictive simulations of hemiparetic gait*. *PLoS Comput. Biol.* **2022**, *18*(9), e1010466. <https://doi.org/10.1371/journal.pcbi.1010466>

34. Falisse, A.; Serrancolí, G.; Dembia, C.L.; Gillis, J.; Jonkers, I.; De Groote, F. *Rapid predictive simulations with complex musculoskeletal models suggest that diverse healthy and pathological human gaits can emerge from similar control strategies*. *J. R. Soc. Interface* **2019**, *16*(157), 20190402. <https://doi.org/10.1098/rsif.2019.0402>

35. Quan, W.; Gao, L.; Wang, S.; Zhou, P.; Zang, Y.; Liu, H.; Zhang, J.; Yang, R.; Fernandez, J.; Gu, Y. *Simulation of Lower Limb Muscle Activation Using Running Shoes with Different Heel-to-Toe Drops Using OpenSim*. *Healthcare* **2023**, *11*(9), 1243. <https://doi.org/10.3390/healthcare11091243>

36. De Groote, F.; Kinney, A.L.; Rao, A.V.; Fregly, B.J. *Evaluation of direct collocation optimal control problem formulations for solving the muscle redundancy problem*. *Ann. Biomed. Eng.* **2016**, *44*(10), 2922–2936. <https://doi.org/10.1007/s10439-016-1591-9>

37. Uhlrich, S.D.; Jackson, R.W.; Seth, A.; Kolesar, J.A.; Delp, S.L. *Muscle coordination retraining inspired by musculoskeletal simulations reduces knee contact force*. *Sci. Rep.* **2022**, *12*, 9842. <https://doi.org/10.1038/s41598-022-13386-9>

38. Kainz, H.; Koller, W.; Wallnöfer, E.; Bader, T.R.; Mindler, G.T.; Kranzl, A.; et al. *A framework based on subject-specific musculoskeletal models and Monte Carlo simulations to personalize muscle coordination retraining*. *Sci. Rep.* **2024**, *14*, 3567. <https://doi.org/10.1038/s41598-024-53857-9>

39. Fregly, B.J.; Meyer, A.J.; Walker, J.A.; Besier, T.F.; Lloyd, D.G.; Delp, S.L. *Grand challenge competition to predict in vivo knee loads*. *J. Orthop. Res.* **2012**, *30*(4), 503–513. <https://doi.org/10.1002/jor.22023>

40. Serrancolí, G.; Falisse, A.; Dembia, C.L.; Vantilt, J.; Tanghe, K.; Lefebvre, D.; Jonkers, I.; De Groote, F. *Subject-exoskeleton contact model calibration leads to accurate interaction force predictions*. *IEEE Trans. Neural Syst. Rehabil. Eng.* **2019**, *27*(8), 1597–1605. <https://doi.org/10.1109/TNSRE.2019.2924536>

41. Promsri, A.; Deedphimai, S.; Promthep, P.; Champamuang, C. *Impacts of Wearable Resistance Placement on Running Efficiency Assessed by Wearable Sensors: A Pilot Study*. *Sensors* **2024**, *24*(13), 4399. <https://doi.org/10.3390/s24134399>

42. Wu, J.; Liu, Y.; Wu, X. *Early Identification of Gait Asymmetry Using a Dual-Channel Hybrid Deep Learning Model Based on a Wearable Sensor*. *Symmetry* **2023**, *15*(4), 897. <https://doi.org/10.3390/sym15040897>

43. Abdullah, M.; Hulleck, A.A.; Katmah, R.; Khalaf, K.; El-Rich, M. *Multibody dynamics-based musculoskeletal modeling for gait analysis: A systematic review*. *J. NeuroEng. Rehabil.* **2024**, *21*, 178. <https://doi.org/10.1186/s12984-024-01458-y>

44. Delp, S.L.; Anderson, F.C.; Arnold, A.S.; Loan, P.; Habib, A.; John, C.T.; Guendelman, E.; Thelen, D.G. OpenSim: Open-source software to create and analyze dynamic simulations of movement. *IEEE Trans. Biomed. Eng.* **2007**, *54*(11), 1940–1950. <https://doi.org/10.1109/TBME.2007.901024>
45. Thelen, D.G.; Anderson, F.C. Using computed muscle control to generate forward dynamic simulations of human walking from experimental data. *J. Biomech.* **2006**, *39*(6), 1107–1115. <https://doi.org/10.1016/j.jbiomech.2005.02.010>
46. Vincent, H.K.; Popp, R.; Cicilioni, O.; Vincent, K.R.; Pezzullo, L.; Martenson, M.; Nixon, R.M. *Reference biomechanical parameters and natural asymmetry among runners across the age spectrum without a history of running-related injuries*. *Frontiers in Sports and Active Living* **2025**, *7*, 1560756. <https://doi.org/10.3389/fspor.2025.1560756>
47. Zadpoor, A.A.; Nikooyan, A.A. *The relationship between lower-extremity stress fractures and the ground reaction force: A systematic review*. *Clin. Biomech.* **2011**, *26*(1), 23–28. <https://doi.org/10.1016/j.clinbiomech.2010.08.005>
48. Brown, A.M.; Zifchock, R.A.; Hillstrom, H.J. *The effects of limb dominance and fatigue on running biomechanics*. *Gait & Posture* **2014**, *39*(3), 915–919. <https://doi.org/10.1016/j.gaitpost.2013.12.007>
49. Forelli, F.; Moiroux-Sahraoui, A.; Labib, M.; Cerrito, A. *Gastrocnemius activation deficits and running biomechanics after anterior cruciate ligament reconstruction: the missing link?* *Frontiers in Sports and Active Living* **2025**, *7*, (article 1594247). <https://doi.org/10.3389/fspor.2025.1594247>
50. Dos'Santos, T.; Bishop, C.; Thomas, C.; Comfort, P.; Jones, P.A. *The effect of limb dominance on change of direction biomechanics: a systematic review of its importance for injury risk*. *Phys. Ther. Sport* **2019**, *37*, 179–189. <https://doi.org/10.1016/j.ptsp.2019.04.005>
51. Brambilla, C.; Beltrame, G.; Marino, G.; Lanzani, V.; Gatti, R.; Portinaro, N.; Molinari Tosatti, L.; Scano, A. Biomechanical Analysis of Human Gait When Changing Velocity and Carried Loads: Simulation Study with OpenSim. *Biology* **2024**, *13*, 321. <https://doi.org/10.3390/biology13050321>
52. Buchanan, S., & Ting, L. *Patterns of asymmetry and energy cost generated from predictive simulations of hemiparetic gait*. *PLoS Comput. Biol.* **2022**, *18*(9), e1010466. <https://doi.org/10.1371/journal.pcbi.1010466>
53. Valente, G.; Pitto, L.; Testi, D.; Seth, A.; Delp, S.L.; Stagni, R.; Viceconti, M.; Taddei, F. *Are subject-specific musculoskeletal models robust to the uncertainties in parameter identification?* *PLoS ONE* **2014**, *9*(11), e112625. <https://doi.org/10.1371/journal.pone.0112625>

**Disclaimer/Publisher's Note:** The statements, opinions and data contained in all publications are solely those of the individual author(s) and contributor(s) and not of MDPI and/or the editor(s). MDPI and/or the editor(s) disclaim responsibility for any injury to people or property resulting from any ideas, methods, instructions or products referred to in the content.